RESEARCH ARTICLE





Three hundred years of snowpack variability in southwestern British Columbia reconstructed from tree-rings

Bryan J. Mood¹ | Bethany Coulthard² | Dan J. Smith¹

¹University of Victoria Tree-Ring Laboratory, Department of Geography, University of Victoria, Victoria, British Columbia, Canada ²Department of Geoscience, University of

²Department of Geoscience, University of Nevada – Las Vega, Las Vegas, Nevada

Correspondence

Bryan J. Mood, University of Victoria Tree-Ring Laboratory, Department of Geography, University of Victoria, Victoria, British Columbia V8W 3R4, Canada. Email: bryan.mood@usask.ca

Funding information

National Science and Engineering Research Council; National Science Foundation Paleo Perspectives on Climate Change Program (NSF 17-582, award #180399)

Abstract

Recent snow droughts in southwestern British Columbia (BC), Canada, have reduced seasonal streamflow during the typically dry late-spring and summer months, leading to socio-economic and ecological impacts that draw attention to the impending consequences of climate change. Knowledge of annual winter snowfall variability within this region is largely derived from a sparse network of short-duration (≤50 years) snow survey stations. In this paper, we develop an annual April 1 snow water equivalent (SWE) reconstruction from living tree-ring chronologies that offer a perspective on long-term natural snowpack variability. The dendrohydrological model estimates the first principal component April 1 SWE for the southwestern regions of BC to 1711. Spectral analysis identified dominant multidecadal April 1 SWE variability over the pre-instrumental period. The reconstruction successfully captures known instrumental period influences of La Niña oscillations on reconstructed SWE, suggesting that our tree-ring based the reconstruction has the potential to provide insights on pre-instrumental ocean-atmosphere links with southwestern BC snowpack dynamics. Runs analysis suggests pre-instrumental snow droughts have been more than twice as long in duration and severity than during the observed period which indicates the instrumental record may not capture the full range of April 1 SWE variability. The reconstruction provides the first high-resolution description of SWE over the past 300 years in southwestern BC and is of immediate use to regional water resource managers.

KEYWORDS

British Columbia, dendroclimatology, hydrology, paleoclimate, snow water equivalent, snowpack

1 | INTRODUCTION

Hydrological Processes. 2020;34:5123-5133.

Winter snowpack plays a critical role in the dynamics of regional hydrologic regimes in many drainage basins in the Pacific Northwest region of North America (Islam, Dery, & Werner, 2017; Mote, Li, Lettenmaier, Xiao, & Engel, 2018; Thakur et al., 2020). Most watersheds in the region support limited storage capacity from natural lakes and human-made reservoirs, and annual runoff variability is related to broad-scale climate oscillations (Abatzoglou, 2011; Bonsal & Shabbar, 2008; Yu & Zwiers, 2007). By storing winter precipitation

into the late-spring and early-summer, snowpacks in these basins supplement water supplies at a time of year when the ecological, social, and industrial demands are greatest (Mote, Hamlet, Clark, & Lettenmaier, 2005; Mote et al., 2018; Rodenhuis, Bennett, Werner, Murdock, & Bronaugh, 2009). Annual snowpacks are, however, vulnerable to changes in climate that influence both cover and depth (Abatzoglou, 2011; Mote et al., 2018). There is concern that recent snowpack declines in the British Columbia (BC) Coast Mountains, Canada, are an outcome of climate change and will persist into the future (Dery, Hernandez-Henriques, Burford, & Wood, 2009; Dery,

Hernandez-Henriques, Owens, Parkes, & Petticrew, 2012; Jost & Weber, 2012; Mote et al., 2018; Rodenhuis et al., 2009).

Water supply for many communities in southwestern BC is dependent upon direct snowmelt contributions to streamflow and reservoir storage, as well as indirectly through contributions to groundwater recharge and throughflow (Beaulieu, Schrier, & Jost, 2012; Eaton & Moore, 2010; Koop et al., 2017; Olmstead, 2014). Record low snowpack totals in 2014 and 2015 contributed to summer-long water supply shortages (aka snow drought; Cook, 2019; Harpold, Dettinger, & Rajagopal, 2017) in the Metro Vancouver region and emphasized the substantial water management challenges that potentially lie ahead for many communities. With further reductions in mountain snowpack certain to result in increasingly severe and frequent summer streamflow droughts (Cook, 2019), focused research is required to describe the full range of natural variability in BC's mountain snowpacks and to understand the underlying relationships to teleconnections with Pacific ocean–atmosphere interactions.

The impact of decreased winter snow delivery and storage in southwestern BC is demonstrated by below-average April 1 SWE totals in recent years. The 2014–2015 winter snowpack in the region was 49% of normal in January and reached a record low of 0% by 1 June (River Forecast Centre, 2017). These low snowpack totals resulted in a severe summer streamflow drought and led to water use restrictions for the 2.6 million people residing in the Metro Vancouver region. Highlighting the importance of mountain snowpacks for sustaining summer streamflow, the depleted runoff had socio-economic and ecological consequences that drew attention to the impending consequences of ongoing climatic changes in this region (Cook, 2019; Fleming & Weber, 2012; Mishra & Coulibaly, 2009).

The instrumental record of winter snowpack variability in southwestern BC is derived from a sparse network of short-duration (≤50 years) snow survey stations (Mote et al., 2018; Rodenhuis et al., 2009). As these records offer only limited insight into long-term snowpack variability, attempting to forecast future trends for water supply management purposes is problematic (Rodenhuis et al., 2009). Short records lead to challenges in understanding long-term ranges of natural variability, whether recent low snowpack totals are "extreme" relative to what has occurred in the past, and/or whether observed ocean–atmosphere influences on snowpack were stable over longer time periods.

In this paper, an April 1 snow water equivalent (SWE) record extending over several centuries was reconstructed for southwestern BC from snow-sensitive Pacific silver fir (PSF, Abies amabilis Douglas ex. J. Forbes) and mountain hemlock (MH, Tsuga mertensiana Bong. Carr.) tree-ring chronologies. Both species have been used to reconstruct snow-related components of streamflow on Vancouver Island and for the Columbia River (Coulthard, Smith, & Meko, 2016; Coulthard & Smith, 2016; Littell et al., 2016). As several Pacific ocean-atmosphere oscillations are known to have teleconnections that enhance or diminish snow delivery during the winter months in this region (Rodenhuis et al., 2009; Spry, Kohfeld, Allen, Dunkley, & Lertzman, 2014; Whitfield, Moore, Fleming, & Zawadzki, 2010), we use snow survey station records from coastal regions to examine

relationships between these oscillations and late-spring SWE dynamics. The reconstruction provides the first high-resolution description of April 1 SWE over the past 300 years in southwestern BC and is of immediate use to water resource managers developing strategies and policies required for adaptation to changing mountain snowpack dynamics in the region.

2 | STUDY AREA AND RESEARCH BACKGROUND

The study area includes the Metro Vancouver area and the southern Pacific Ranges extending from Joffre Lakes to the lower Fraser River within the southwestern BC Coast Mountains (Figure 1). Coastal settings in this region are moderated by proximity to the Pacific Ocean and experience short, cool summers and long, wet winters. Average air temperatures 1,000 m above sea level (asl) remain below 0°C for 0-5 months of the year and above 10°C for 1-3 months of the year (Pojar, Klinka, & Meidinger, 1991; Kottek et al., 1996). The study area includes BC's wettest ecological zone with orographic precipitation on the windward slopes of the Pacific Ranges resulting in precipitation totals that range between 1,700 to 5,000 mm/year, with 70% falling as snow and/or rain during the winter months (Pojar et al., 1991; Spry et al., 2014) (Figure 2a). Precipitation totals are substantially less on the eastern (leeward) continental slopes, where persistent rain shadow conditions prevail (Church & Ryder, 2010; Kottek, Friser, Beck, Rudolf, & Rubel, 2006; Moore, Spittlehouse, Whitfield, & Stahl, 2010; Pojar et al., 1991) (Figure 2a,b).

Previous research within the study area identified a causal relationship between April 1 SWE variability and inter-annual/-decadal climate variability generated by ocean-atmosphere interactions originating in the Pacific Ocean (Sellars, Garret, & Woods, 2008; Spry et al., 2014; Whitfield et al., 2010). These interactions include those characterized by the Pacific Decadal Oscillation (PDO), the El Niño-Southern Oscillation (ENSO), and the Pacific North American (PNA) pattern (Abatzoglou, 2011; Mote et al., 2018; Rodenhuis et al., 2009; Thakur et al., 2020). Warm/cool phase relationships between SWE and ENSO show that an annual variability of greater than 30% characterized the interval between 1951 and 2007 (Rodenhuis et al., 2009). Relationships between SWE and PDO variability are less pronounced over the instrumental period, with a 15% change in snowpack noted between warm/cool phases (Rodenhuis et al., 2009). The PDO is a large-scale climate system that influences the surface climate and hydrology of western North America and is typically coupled with ENSO when describing regional temperature and precipitation regimes (Rodenhuis et al., 2009; Whitfield et al., 2010). In the South Coast BC region precipitation is typically higher during cool phases of PDO and lower during warm phases (Kiffney, Bull, & Feller, 2002; McCabe & Dettinger, 2002; Moore & Kendry, 1996; Stahl, Moore, & Mckendry, 2006), although the role of PDO on western US winter climate can be inconsistent (McAfee, 2014; Cook et al., 2018). The PNA affects the overall hydroclimate of southwestern BC through changes in winter storm intensity and frequency (Rodenhuis et al., 2009). No

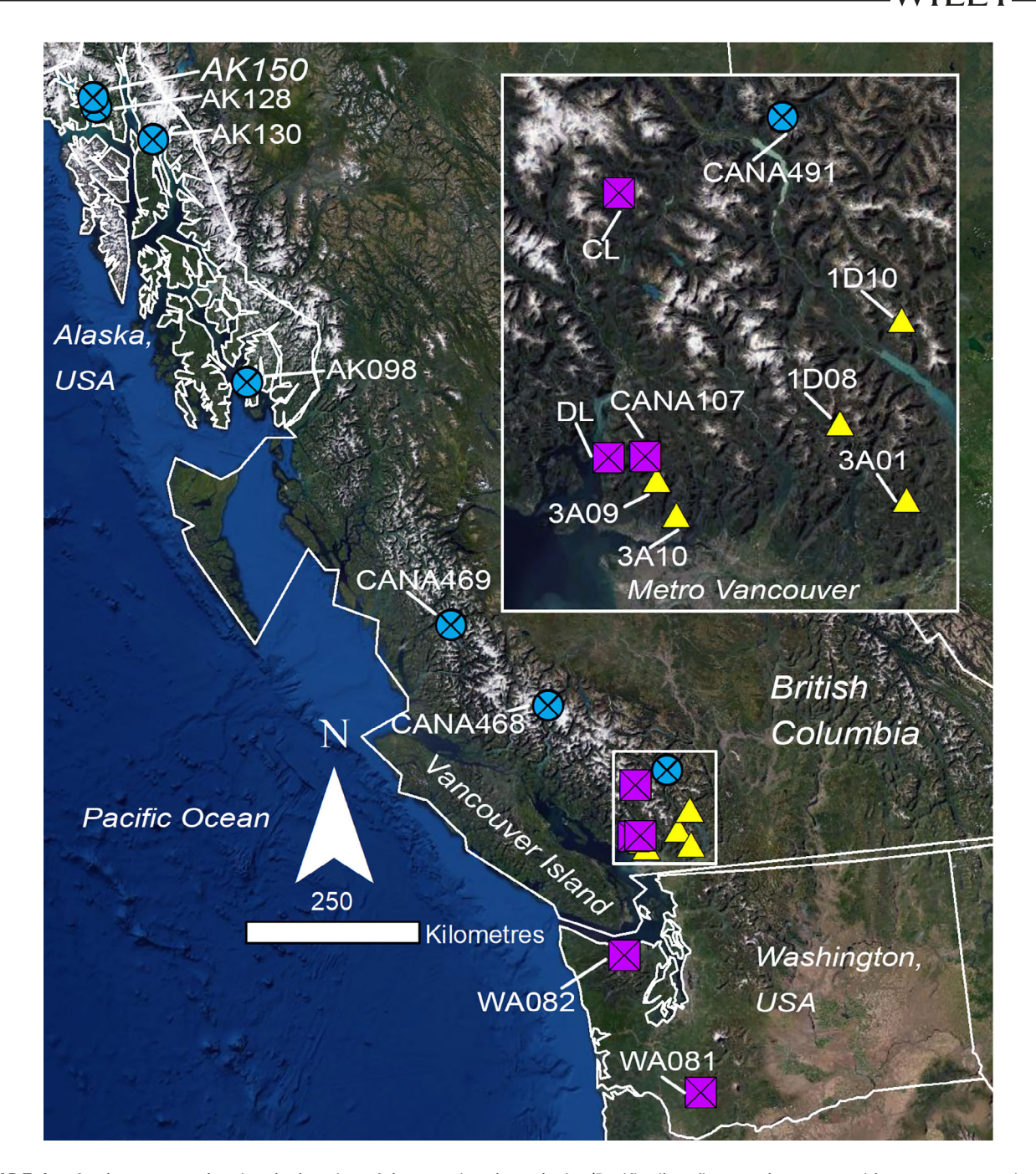


FIGURE 1 Study area map showing the location of the tree-ring chronologies (Pacific silver fir = purple squares with crosses; mountain hemlock = blue circles with crosses) and snow survey stations (yellow triangles) incorporated into this research. The inset map shows the snow survey stations and regional-scale tree-ring chronologies in more detail. The area it focuses on is outlined in the larger map

statistical relationships between SWE variability and the PNA are confirmed in the BC Coast Mountains, although it has been associated with the seasonal snow line elevation (Abatzoglou, 2011).

3 | METHODS

MH and PSF are conifer tree species common to maritime climate regions in Pacific North America (Crawford & Oliver, 1990). Normally found at sites with deep, well-drained soils at high elevations, they are

often found in association with other tree species including western hemlock (*Tsuga heterophylla*), yellow-cedar (*Chamaecyparis nootkatensis*), and western red cedar (*Thuja plicata*) (Pojar et al., 1991).

Snow persisting into the summer truncates the growing season of many tree species located close to treeline (Ettinger, Ford, & HilleRisLambers, 2011). At high elevation sites, PSF tends to grow where annual precipitation totals range from 750 to over 6,500 mm/ year (Crawford & Oliver, 1990). Near the upper limit of this altitudinal range, their annual radial increments are known to be limited by latelying snowpack persisting into the summer growing season

(Crawford & Oliver, 1990; Ettinger et al., 2011). MH trees share similar environmental requirements and, due to their strong, negative relationship to snowpack depth, have previously been used to reconstruct snowpack and other hydroclimatic characteristics in Pacific North America (e.g., Appleton & St. George, 2018; Coulthard et al., 2016; Coulthard & Smith, 2016; Pederson et al., 2011; Peterson & Peterson, 2001; Welsh, Smith, & Coulthard, 2019). By comparison, PSF has seen limited use as an environmental proxy (e.g., Littell et al., 2016), although in limited cases it has demonstrated stronger statistical relationships to April 1 SWE at some high elevation sites in the Pacific Northwest (Ettinger et al., 2011).

3.1 | Tree-ring data

The tree-ring width data used in the research originated from field sampling or was downloaded from the International Tree-Ring Data Bank (ITRDB; NOAA, 2017). Mixed-age PSF tree ring samples were collected with 5.2-mm increment borers using standard dendrochronological sampling techniques (two samples per tree from 20 different trees; Fritts, 1976; Speer, 2010) at high-elevation sites in southwestern BC in the summer of 2016. Mixed-age samples were collected to

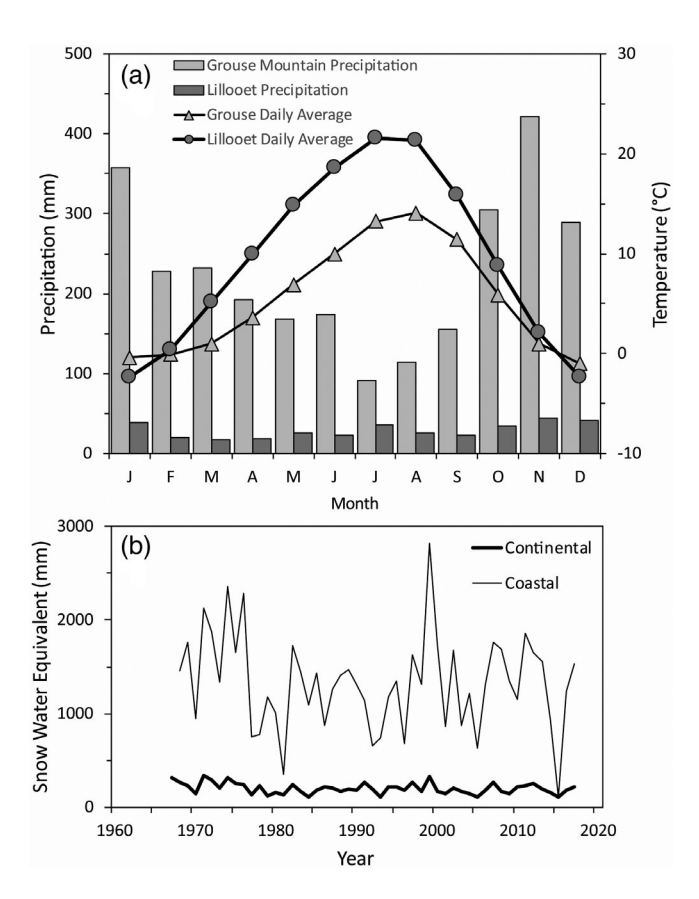


FIGURE 2 General climate information for the study region. (a) Climate normal (1981–2010) for coastal (Grouse Mountain, station ID: 1105658) (Environment and Climate Change Canada, 2017) (b) time series of average coastal April 1 SWE record (River Forecast Centre, 2017)

allow for the potential use of regional-curve standardization techniques that account for age-related growth trends across series (Briffa & Melvin, 2011). After air drying and processing, the annual ring widths of the cores were measured, to the nearest 0.01-mm, at the University of Victoria Tree-Ring Laboratory (UVTRL) using a WinDendro™ digital measurement system (v. 2016a; Guay, Gagnon, & Morin, 1992). Once measured, the two samples from the same tree were visually and statistically crossdated using dplR (Bunn, 2008).

Crossdated PSF and MH tree-ring measurements from several supplementary sample sites were downloaded from the ITRDB. The sites were selected for their proximity to the study region, age span, and relatively high-elevation locations, as well as sensitivity to Pacific sea-surface temperatures and teleconnections (B. Black, personal communication, 2019).

All tree-ring measurements were converted to standardized indices using the R package dpIR (Bunn, 2008). We used a negative exponential growth curve to remove age-growth-related trends and retain annual- to decadal-scale variability typically associated with teleconnections to Pacific Ocean oscillations. Where individual series lacked exponential fit, we fit a horizontal line through the arithmetic mean. We took a conservative approach to autocorrelation in the tree-ring chronologies, using the residual chronologies rather than standardized chronologies which contained unknown sources of persistence. While standard chronologies are sometimes used in dendrohydrological reconstructions of streamflow where watersheds have long concentration times (e.g., Gray et al., 2011; Littell et al., 2016; Woodhouse et al., 2016), the regional snowpack record used for this analysis did not contain significant autocorrelation (see Figure 3).

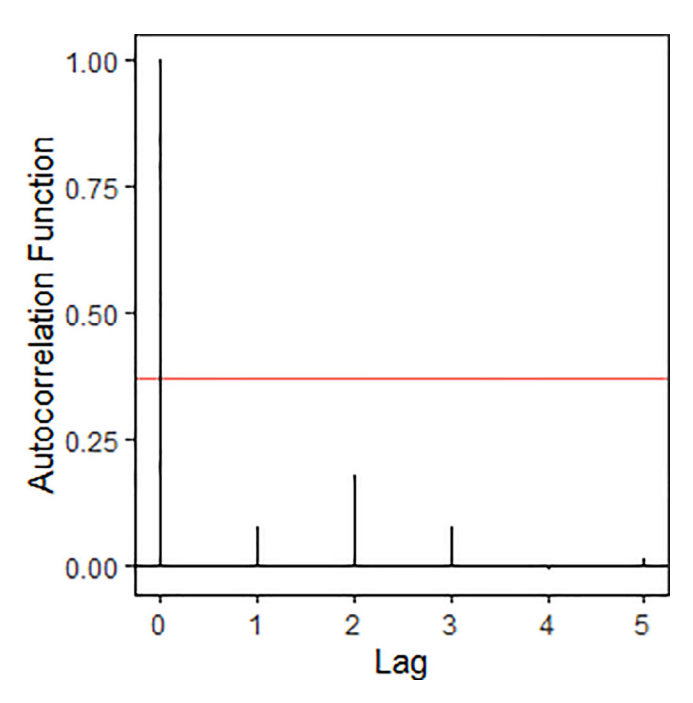


FIGURE 3 Autocorrelation function plots for April 1 SWE PC. The red line represents the 99% confidence interval. Values exceeding the red line indicate significant autocorrelation

Following construction of our site-specific chronologies, intercorrelated tree-ring chronologies were combined by species using Principal Component Analyses (PCA) based on the correlation matrix to extract the underlying variability associated with growth across the selected PSF and MH sites, respectively. Similar to other tree-ring-based reconstructions using PCA in our region, only the first component explaining the most variance was used as a candidate predictor in our model (Coulthard et al., 2016; Littell et al., 2016; Welsh et al., 2019).

3.2 | SWE data

SWE data from snow survey stations located in southwestern BC were accessed using the online portal managed by the BC River Forecast Centre (River Forecast Centre, 2017). April 1 SWE records exceeding 45 years in length (to maximize the model calibration period) were downloaded, and long-term means used to replace missing values. Where missing values exceeded 10%, the record was discarded. April 1 SWE sites were entered into a PCA on the correlation matrix to extract the underlying regional variance, with only the leading principal component used for further analysis. The component was tested for significant autocorrelation using the "acf" function in R (Bretherton, Smith, & Wallace, 1992; North, Bell, Cahalan, & Moeng, 1982).

3.3 | Model estimation

Pearson's correlation coefficients were calculated between the April 1 SWE records and the tree-ring principal components to determine whether linear relationships exist between the proxies and lateseason snow. Tree-ring principal components that were significantly correlated to April 1 SWE were used as model predictors and entered into a multiple linear regression model estimating regional SWE. Models were evaluated based on adjusted R², multicollinearity (variance inflation factor or VIF), autocorrelation at lag 1 (Durbin-Watson or DW), and cross-validation statistics (Reduction of Error or RE). Adjusted R^2 is a modified version of R^2 that accounts for the number of variables in the model and describes the explanatory power of the model (Fritts, 1976). Multicollinearity refers to the degree which our model predictors are linearly associated and how much variance may be inflated (Cook & Pederson, 2011). The DW test is used to detect the presence of first-order autoregressive processes in the time series (Durbin & Watson, 1950, 1951). Our cross-validation was conducted using the split-k and leave-one-out (LOO) methods to determine the RE statistic. Any model where RE > 0 is considered to have skill and appropriate for use (Panthi, Brauning, Zhou, & Fan, 2017). The split-k method subdivides the data into k subsets to use as training data which is repeated k times. The LOO method is similar to split-k where k is equal to sample size. (Wong, 2015). Given the relatively low sample depth of our data for training, we used both methods to support our model outputs.

3.4 | Analysis of the reconstruction

Reconstructed and instrumental April 1 SWE were compared with measured seasonal and annual ENSO, PDO, and PNA climate oscillation indices (October of the previous year to March) during the instrumental period to determine whether the reconstruction captures the SWE variability known to characterize the indices. While there are several ENSO-related indices, in this study we used the extended bimonthly multivariate ENSO index (MEI) which employs five variables to produce a time series of ENSO conditions over the instrumental record (Wolter & Timlin, 1993, 2011). We used this index as: (a) it utilizes multiple variables to create an ENSO index; (b) it was employed by previous studies in our region; and (c) the MEI extends from 1871 to present making it the longest available index for use. A difference-of-correlations test was conducted on both the SWE observations, as well as on the reconstructed values, against positive and negative phases of the climate oscillations.

We summarized snow drought frequencies and magnitudes for southwestern BC using a runs analysis based on bottom 20th percentile reconstructed snowpack values over the observed and preinstrumental periods, respectively (Meko, Woodhouse, & Bigio, 2017; Salas, Delleur, Yevjevich, & Lane, 1980). A Morlet wavelet analysis using the R-package WaveletComp (Roesch & Schmidbauer, 2015) was also used to identify fluctuations in power over the length of the full reconstruction period.

4 | RESULTS

A regional SWE record was developed from stations located in coastal southwestern BC based on the first principal component (PC1) of instrumental April 1 SWE, which captured 89% of the observed April 1 SWE variance (Table 1) and did not contain autocorrelation (Figure 3). Five significantly intercorrelated PSF chronologies were selected for use as snowpack proxies in this study (Table 2). The chronologies had RBARs ranging from 0.350 to 0.491 and were significantly correlated with April 1 SWE (Table 3). Erring on the conservative side, negative exponential detrending was used than regional curve standardization to avoid the "differing contemporaneous growth rate" problem (Briffa & Melvin, 2011). Because the snowpack variability of interest in this study is a relatively high- to mediumfrequency process, potential loss of lower-frequency signal due to the application of negative exponential detrending to differently-aged tree-ring chronologies (e.g., the "segment length curse"; Cook, Briffa, Meko, Graybill, & Funkhouser, 1995) was considered acceptable. The chronologies were entered into a PCA, with only the first principal component from this group capturing >10% of variance (PSFPC1, 55.1%) and used as a model predictor. Use of PSFPC1 instead of individual chronologies as model predictors enhanced the explanatory power of the reconstruction but restricted the reconstruction period to 1710-1992.

Seven site-level MH chronologies from Alaska and BC, with RBARs ranging from 0.437 to 0.502, were also entered into a PCA.

TABLE 1 Descriptive information of manual snow survey stations used in this study. Records were collected from the BC River Forecast Centre (2017) website. Station ID is associated with BC River Forecast designations; Coordinates (latitude and longitude) are in decimal degrees; Elevation is rounded to the nearest 10 m above sea level; Mean April 1 SWE is calculated across the whole time series; Span is the length of continuous April 1 SWE measurements from each station; Length is the total number of years available for analysis; Explained variance represents the explanatory power of the first principal component from the PCA analysis conducted on the snowpack records

Station ID	Latitude (DD)	Longitude (DD)	Elevation (m asl)	Mean April 1 SWE	Span (years)	Length (years)	Explained variance
1D08	49.58	-122.32	1,195	1,529	1968-2014	46	
1D10	49.83	-122.06	1,555	1,360	1968-2014	46	
3A01	49.38	-122.08	1,130	1,231	1936-2014	78	
3A09	49.46	-123.03	880	1,479	1946-2014	68	
3A10	49.37	-122.96	1,010	1,235	1945-2014	69	
							89%

TABLE 2 Tree-ring chronology information. Species/type are bold and italics represents time series used as predictors in the reconstruction. Tree-ring site numbers in brackets are ITRDB codes. RBAR is the average value across whole index; length is the span of years available for analysis

Study site (site code)	Source	Lat (DD)	Lon (DD)	Elevation (m asl)	RBAR	Length
Pacific silver fir						
Deek's Lake (DL)	This study	49.52	-123.21	1,050	0.350	1,696-2015
Callaghan Lake (CL)	This study	50.18	-123.13	975	0.360	1,696-2015
Seymour Basin (CANA107)	Dobry et al. (1996)	49.52	-123.07	1,000	0.491	1,686-1992
Hurricane ridge (WA081)	Schweingruber, Briffa, and Jones (1991)	46.15	-122.15	1,200	0.372	1,698-1983
Mt. St. Helens (WA082)	Schweingruber et al. (1991)	47.98	-123.47	1,200	0.437	1,648-1980
Pacific silver fir principal compo	onent				Explained variance	
Component 1 (PSFPC1)					55.1%	1,698-1992
Mountain hemlock						
Joffre Lake (CANA491)	Wood and Smith (2011)	50.35	-122.48	1,430	0.437	1711-2012
Cathedral glacier (CANA468)	Larocque and Smith (2005)	51.24	-124.87	1,360	0.490	1,682-2010
M Gurr Lake (CANA469)	Pitman and Smith (2012)	52.28	-126.89	1,310	0.502	1,673-2000
Deer mountain (AK098)	Wiles, Jacoby, and Davi (1999)	55.3	-131.6	810	0.491	1935-1999
Repeater Station (AK128)	Jarvis, Wiles, Appleton, D'Arrigo, and Lawson (2013)	58.62	-135.87	720	0.453	1,695-2009
Juneau Mountain (AK130)	Jarvis et al. (2013)	58.3	-134.38	540	0.437	1710-1999
Wright Mountain (AK150)	Wiles et al. (2014)	58.74	-135.98	640	0.456	1710-2010
Mountain hemlock principal component					Explained variance	
Component 1 (MHPC1)					53.1%	1711-1999

The first two principal components from this group explaining 53.1% and 20.8% of variance, respectively, and spanned the interval from 1711 to 1999 (Table 2). Only the first principal component (MHPC1) was significantly correlated with April 1 SWE PC1 (Table 3) and used as a model predictor.

A stepwise linear regression model was used to estimate snowpack for both study regions using PSFPC1 and MHPC1 as candidate model predictors, resulting in the reconstruction equation:

Southwestern BC April 1 SWE_{PC} = -0.69*MHPC1 + -0.34*PSFPC1 + -0.30 ± 0.66 .

The April 1 SWE reconstruction extends from 1711 to 1992 and explains 50% of the variance in the coastal April 1 SWE PC, accounting for lost degrees of freedom. The model has a DW statistic of 2.54, VIF of 1.42, and F-Ratio of 13.32 (Table 4). It was successfully cross-validated using both LOO (RE = 0.23) and split-k (RE = 0.43) methods. Regression and cross-validation statistics are shown in Table 4 and a time plot of the instrumental, reconstructed, and cross-validated coastal snowpack is shown in Figure 4. The full reconstruction is also illustrated in Figure 4.

To assess the ability of the reconstruction to capture past variability associated with large-scale ocean-atmosphere teleconnections

over common periods, a difference-of-correlations test between the reconstructed and instrumental datasets and ENSO was completed. Instrumental coastal snowpack was significantly correlated with negative phases of ENSO at seasonal and annual scales (Table 5). Reconstructed coastal snowpack was significantly correlated with seasonal measurements of negative ENSO (Table 5).

The runs analysis identified 12 multi-year snow droughts in the reconstruction prior to the instrumental record at 1719–1723 (5 years), 1766–1767 (2 years), 1791–1793 (3 years), 1803–1805 (3 years), 1816–1817 (2 years), 1885–1886 (2 years), 1891–1892 (2 years), 1901–1902 (2 years), 1904–1905 (2 years), 1914–1915

TABLE 3 Pearson correlations between model parameters used in the reconstruction

Time series	April 1 SWE PC
Pacific silver fir component 1 (PSFPC1)	-0.65
Mountain hemlock component 1 (MHPC1)	-0.64

TABLE 4 Reconstruction, cross-validation, and descriptive statistics

Reconstruction	R ²	Adj. R ²	D-W	VIF	SE	F-ratio
April 1 SWE PC	0.54	0.50	2.54	1.42	0.72	13.32
Cross validation	Leave-one-out RE	Spilt-k RE	RMSE			
Coastal	0.23	0.43	0.66			

Abbreviations: DW, Durbin-Watson Statistic; VIF, variance inflation factor; RE, reduction of error; RMSE, root mean squared error.

Notes: Two different cross-validation calculations were used to verify our model. The first, leave-one-out divides the data the same number of times as samples for validation while split-k divides the data in half.

(2 years), 1934–1935 (2 years), and 1941–1942 (2 years) with 22 other single-year events (Figure 5). In contrast, over the instrumental period, only one multi-year snow drought from 1980 to 1981 (2 years) and three other single-year events (1978, 1986, and 1993) occurred. The highest magnitude snow drought over the entire reconstruction was documented in 1914–1915 (Z-score = -1.6) while the highest magnitude snow drought over the instrumental period occurred in 1982 (-1.1). A Morlet wavelet analyses identified significant variability for reconstructed and instrumental coastal snowpack at 45- to 60- and 68- to 73-year frequencies (Figure 6a and b).

5 | DISCUSSION

Our reconstruction model of April 1 SWE explains 50% of the observed SWE variance. As is the case in other parts of western North America (Mote et al., 2018), the findings show that both instrumental and reconstructed snowpack are associated with ENSO during the observed period.

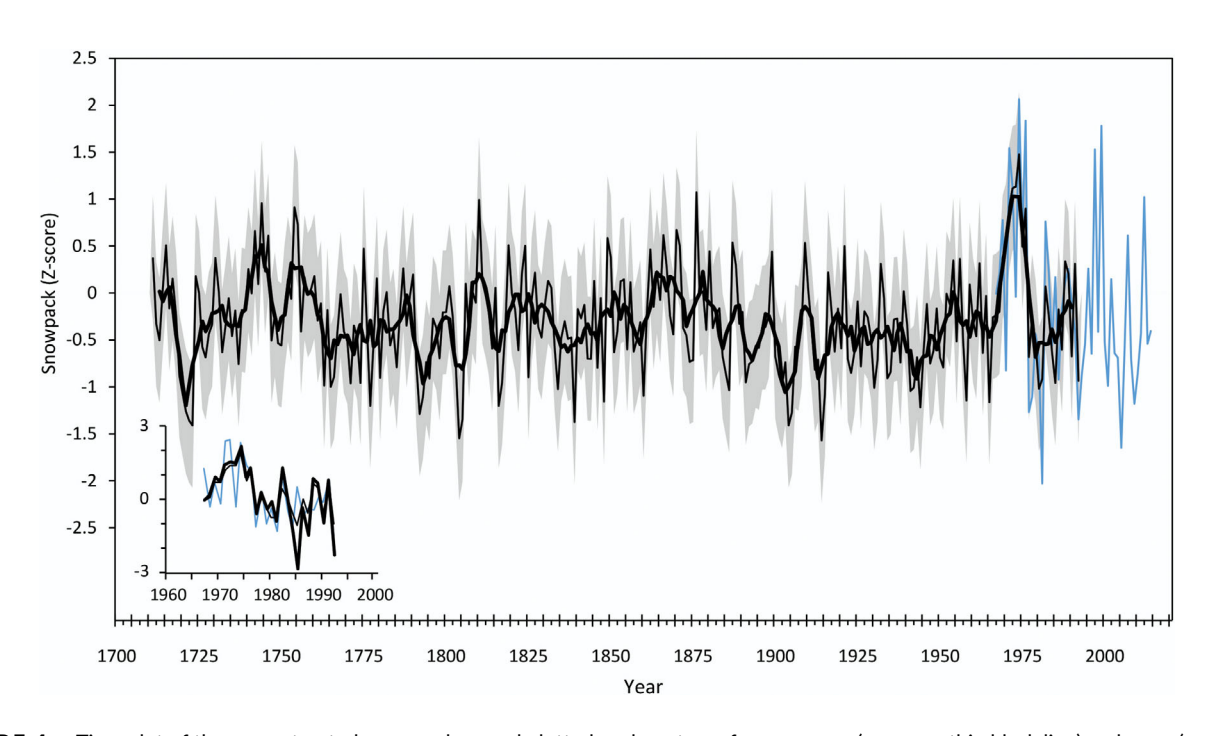


FIGURE 4 Time plot of the reconstructed snowpack record plotted as departures from average (z-scores; thin black line) and error (grey area) calculated from the cross-validation RMSE. The thick black line is a 5-year running mean. The smaller inset line graph below the reconstruction is a time plot of the instrumental snowpack principal component (blue), reconstructed (thick black), and cross-validated (thin black) records

TABLE 5 Seasonal difference-of-correlations test results describing the relationship between coast snowpack and El Niño-Southern Oscillation (ENSO)

	Time period									
Туре	DJF		MAM		JJA		SON		Annual	
	+	-	+	-	+	-	+	-	+	-
Instrumental		-0.63		-0.77	0.53	-0.49	0.57		0.50	-0.58
n		18		12	22	17	22		23	16
Reconstructed		-0.26		-0.35		-0.24		-0.28		
n		65		64		64		63		

Notes: ENSO indices were grouped into negative and positive values then correlated to both the calculated (instrumental) and modelled (reconstructed) SWE. Values shown are p < .05 while **bold** values indicate p < .01. Nonsignificant correlations are not reported.

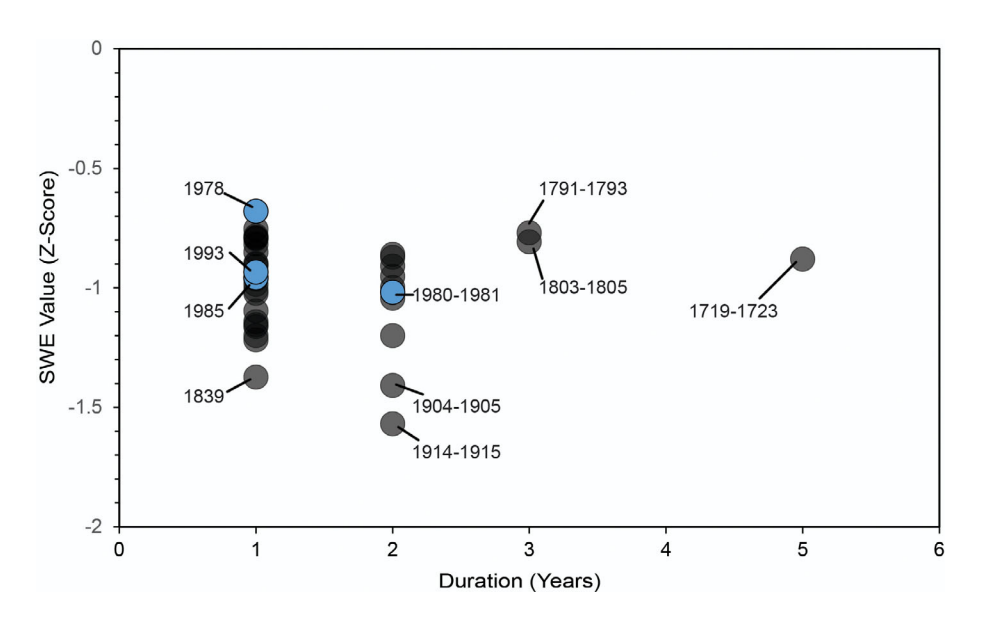


FIGURE 5 Scatterplot of runs analysis snow drought magnitudes and durations (bottom 20th percentile). Grey markers represent pre-instrumental period events and blue markers indicate events during the observational period

The first principal component of the PSF chronologies serves as a proxy for snowpack as deep or late-lying snowpacks typically result in a truncated growing season and the growth of a narrow annual ring in PSF (Ettinger et al., 2011). While a growing number of high-elevation paleoenvironmental reconstructions in western North America use MH radial growth trends as a proxy for snowpack and/or dry-season streamflow (e.g., Appleton & St. George, 2018; Coulthard et al., 2016; Pederson et al., 2011; Wood, Smith, & Demuth, 2011), there is evidence that PSF may be more sensitive to SWE at some sites and demonstrate higher growth synchrony across populations at a broader range of elevations (Ettinger et al., 2011). The robustness of PSF in our reconstruction serves to highlight its potential as a snowpack proxy, perhaps providing an independent record for validating reconstructions in the study region that primarily rely upon MH tree-ring records (e.g., Coulthard et al., 2016; Wood et al., 2011).

Both instrumental and reconstructed coastal snowpack reflect the influence of known ocean-atmosphere teleconnections on April 1 SWE during the instrumental period, an indication that these and other tree-ring-based SWE reconstructions in the study region have the ability to capture pre-instrumental SWE-dynamics driven by these modes. Both snowpack records were most strongly linked with negative phases of ENSO (La Niña) events (Table 5). These events typically coincide with cooler and wetter winters in southwestern BC that tend to promote higher-than-average winter snowpack (Rodenhuis et al., 2009) and higher streamflow discharge totals in western Canada (Whitfield et al., 2010). The reconstructed record is weakly associated with PDO during winter (DJF) and spring (MAM; Table 5), and demonstrates interdecadal spectral variability similar to fluctuations observed in the PDO over the last 300 years (Figure 6a; Mac-Donald & Case, 2006; Buckley et al., 2019). While the PDO is typically associated with multidecadal climate variability in the study region, its influence is less pronounced than that of ENSO (Rodenhuis et al., 2009). Our results are largely consistent with streamflow reconstructions derived from snow-sensitive trees on Vancouver Island, BC, that captured similar instrumental-period phase changes related to PDO and ENSO (Coulthard et al., 2016; Coulthard & Smith, 2016).

Runs analysis suggests snow droughts in southwestern BC can be more severe in both duration and magnitude than instrumental data have shown. Pre-instrumental snow droughts lasted up to 5 years in

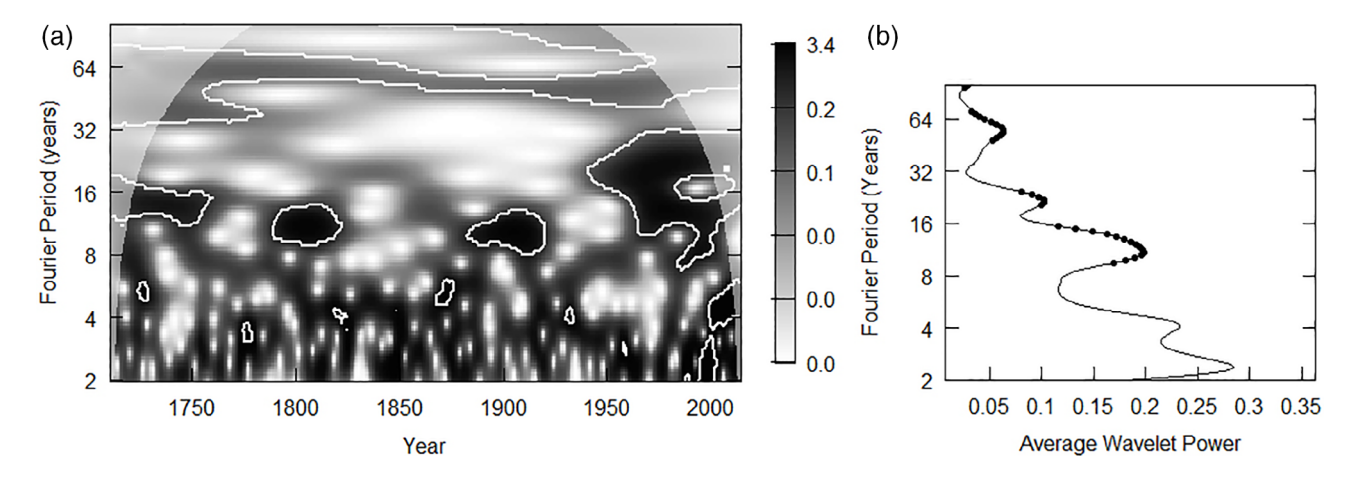


FIGURE 6 (a) Morlet wavelet power spectrums of the April 1 SWE PC reconstruction. The y-axis represents Fourier periods while the x-axis represents time. White enclosed areas represent a 95% confidence interval where significant wavelengths in the series are detected. The lower contrast, or faded, areas on the left and right extremes of each figure represent areas outside of the analysis that is susceptible to zero padding effects. Part (b) presents average wavelet power through time at different Fourier periods. The calculated value is average of each Fourier period across the entire examined time series. Black circles indicate intervals where power averages are significant across the entire time series

duration (1719–1723), while observed snow droughts lasted a maximum of 2 years (only one event in 1980–1981). In contrast, two-year snow droughts are common in the pre-instrumental period (9 events).

5.1 Usefulness in water policy and management

Melting seasonal snowpacks provide an important contribution to streamflow runoff and water supply in southwestern BC during the dry summer months (Moore et al., 2010). In particular, snowpack is often correlated with overall summer supply for many of the streams in the region (Bealieu et al., 2002). The high-resolution snowpack reconstructions developed in this research demonstrate the potential for contextualizing recent low snowpack events over those characterizing the past three centuries. We provide a new, longer-term context of snow droughts in southwestern BC and show that these events can be much more severe and longer in duration than previously documented, and under non-anthropogenically forced conditions. These long-term records can help water managers to more accurately calculate probabilities of future high and low SWE years, and related freshet and drought dynamics. They cannot, however, directly account for the influences of spring and summer temperature on snowmelt.

6 | CONCLUSIONS

We present the first multi-century, annual-resolution record of snow-pack variability for southwestern BC based on tree-ring width data from PSF and MH trees. Our reconstruction portrays regionally relevant snowpack patterns, differences in variability, and the influence of ENSO on snowpack variability during the instrumental period. It also shows that in the past, snow droughts were up to twice as long duration and twice as severe in magnitude than snow droughts in the

observed record. Importantly, these past and more severe snow droughts represent long-term natural variability in the snowpack system and were not additionally influenced by anthropogenic climate change. Wavelet analysis suggests our reconstruction may also capture the influence of Pacific Ocean oscillations across the full reconstructed period. The reconstruction highlights the potential for developing pre-instrumental annual and/or seasonal snowpack records in BC that are relevant for developing water management policies.

ACKNOWLEDGEMENTS

The authors wish to thank two anonymous reviewers, M. Pisaric, D. Atkinson, and T. Gardner for comments on early versions of the manuscript. Financial support for the research was provided by the Natural Science and Engineering Research Council's (NSERC) Discovery Grant (Smith) and NSERC Canadian Graduate Scholarship (Mood). The authors declare no conflict of interest.

DATA AVAILABILITY STATEMENT

The data that support the findings of this study are openly available in the International Tree-Ring Data Bank (ITRDB) using the associated site code (see Table 2).

ORCID

Bryan J. Mood https://orcid.org/0000-0001-8266-8853

REFERENCES

Abatzoglou, J. T. (2011). Influence of the PNA on declining mountain snowpack in the western United States. *International Journal of Clima*tology, 31, 1135–1142.

Appleton, S. N., & St. George, S. (2018). High-elevation mountain hemlock growth as a surrogate for cool-season precipitation in crater Lake National Park, USA. *Dendrochronologia*, 52, 20–28.

Beaulieu M., Schreier H., Jost G. (2012). A shifting hydrological regime: a field investigation of snowmelt runoff processes and their connection

- to summer base flow, Sunshine Coast, British Columbia. *Hydrological Processes*, 26(17), 2672–2682. http://dx.doi.org/10.1002/hyp.9404.
- Beaulieu, M., Schrier, H., & Jost, G. (2012). A shifting hydrological regime: A field investigation of snowmelt runoff processes and their connection to summer base flow, Sunshine Coast, British Columbia. Hydrological Processes, 26, 2672–2682.
- Bonsal, B., & Shabbar, A. (2008). Impacts of large-scale circulation variability on low streamflows over Canada: A review. Canadian Water Resources Journal, 33, 137–158.
- Bretherton, C. S., Smith, C., & Wallace, J. M. (1992). An intercomparison of methods for finding coupled patterns in climate data. *Journal of Climate*, 5, 541–560.
- Briffa, K. R., & Melvin, T. V. (2011). A closer look at regional curve standardization of tree-ring records: Justification of the need, a warning of some pitfalls, and suggested improvements in its application. In M. K. Hughes, T. W. Swetnam, & H. F. Diaz (Eds.), *Dendroclimatology: Progress and prospects* (pp. 113–145). Dordrecht, The Netherlands: Springer.
- Buckley, B. M., Ummenhofer, C. C., D'Arrigo, R. D., Hansen, K. G., Truong, L. H., & Stahle, D. K. (2019). Interdecadal Pacific oscillation reconstructed from trans-Pacific tree rings: 1350-2004 CE. Climate Dynamics, 53, 3181-3196.
- Bunn, A. G. (2008). A dendrochronology program library in R (dpIR). Dendrochronolgia, 25, 115–124.
- Church, M., & Ryder, J. M. (2010). Physiography of British Columbia. In R. G. Pike, T. E. Redding, R. D. Moore, R. D. Winkler, & K. D. Bladon (Eds.), Compendium of forest hydrology and geomorphology in British Columbia Land management handbook (Vol. 66, pp. 17–46). Victoria, Canada.B.C. Ministry of Forests and Range Research Branch.
- Cook, B. I. (2019). Drought: An interdisciplinary perspective (p. 215). New York, NY: Columbia University Press.
- Cook, E. R., Briffa, K. R., Meko, D. M., Graybill, D. A., & Funkhouser, G. (1995). The 'segment length curse' in long tree-ring chronology development for palaeoclimatic studies. *The Holocene*, 5, 229–237.
- Cook, E. R., & Pederson, N. (2011). Uncertainty, emergence, and statistics in dendrochronology. In M. Hughes, T. Swetnam, & H. Diaz (Eds.), Dendroclimatology: Developments in Paleoenvironmental research (Vol. 11, pp. 77–112). Dordrecht, The Netherlands: Springer.
- Cook Benjamin I., Williams A. Park, Mankin Justin S., Seager Richard, Smerdon Jason E., Singh Deepti (2018). Revisiting the Leading Drivers of Pacific Coastal Drought Variability in the Contiguous United States. *Journal of Climate*, 31(1), 25–43. http://dx.doi.org/10.1175/jcli-d-17-0172.1.
- Coulthard, B., & Smith, D. J. (2016). A 477-year dendrohydrological assessment of drought severity for Tsable River, Vancouver Island, British Columbia, Canada. *Hydrological Processes*, 30, 1676–1690.
- Coulthard, B., Smith, D. J., & Meko, D. M. (2016). Is worst-case scenario streamflow drought underestimated in British Columbia? A multicentury perspective for the south coast, derived from tree-rings. *Journal of Hydrology*, 534, 205–218.
- Crawford, P. D., & Oliver, C. D. (1990). Pacific silver fir. In R. M. Burns & B. H. Honkala (Eds.), *Silvics of North America* (pp. 6–25). Washington, D.C.:).United States Department of Agriculture, Forest Science.
- Dery, S. J., Hernandez-Henriques, M. A., Burford, J. E., & Wood, E. F. (2009). Observational evidence of an intensifying hydrological cycle in northern Canada. *Geophysical Research Letters*, 26, L13402.
- Dery, S. J., Hernandez-Henriques, M. A., Owens, P. N., Parkes, M. W., & Petticrew, E. L. (2012). A century of hydrological variability and trends in the Fraser River basin. *Environmental Research Letters*, 7, 024019.
- Dobry, J., Kyncl, J., Klinka, K., & Blackwell, B. A. (1996). Climate signals in coastal old-growth forest trees near Vancouver, British Columbia. In J. S. Dean, D. M. Meko, & T. W. Swetnam (Eds.), Proceedings of the International Conference on Trees, Environmental, and Humanity, Tucson, Arizona, 17–21 May 1994 (pp. 733–741). Tucson, AZ: Radiocarbon, Department of Geosciences, University of Arizona.

- Durbin, J., & Watson, G. S. (1950). Testing for serial correlation in least squares regression, I. *Biometrika*, 37, 408–428.
- Durbin, J., & Watson, G. S. (1951). Testing for serial correlation in least squares regression, II. *Biometrika*, 38, 159–179.
- Eaton, B., & Moore, R. (2010). Regional hydrology. In R. G. Pike, T. E. Redding, R. D. Moore, R. D. Winkler, & K. D. Bladon (Eds.), Compendium of Forest hydrology and geomorphology in British Columbia Land management handbook (Vol. 66, pp. 85–110). Victoria, Canada: Forrex.
- Environment and Climate Change Canada [ECCC]. (2017). Historical data.

 Retrieved from http://climate.weather.gc.ca/historical_data/search_historic_data_e.html
- Ettinger, A. K., Ford, K. R., & HilleRisLambers, J. (2011). Climate determines upper, but not lower, altitudinal range limits of Pacific northwest conifers. *Ecology*, *92*, 1323–1331.
- Fleming, S. W., & Weber, F. A. (2012). Detection of long-term change in hydroelectric reservoir inflows: Bridging theory and practice. *Journal of Hydrology*, 470, 36–54.
- Fritts, H. C. (1976). Tree-rings and climate. London, England: Academic Press. Gray Stephen T., Lukas Jeffrey J., Woodhouse Connie A. (2011). Millennial-Length Records of Streamflow From Three Major Upper Colorado River Tributaries1. JAWRA Journal of the American Water Resources Association, 47(4), 702–712. http://dx.doi.org/10.1111/j.1752-1688.
- Guay, R., Gagnon, R., & Morin, H. (1992). A new automatic tree-ring measurement system based on a line scan camera. Forestry Chronicle, 68, 138–141.
- Harpold, A., Dettinger, M. D., & Rajagopal, S. (2017). Defining snow drought and why it matters. Eos, Earth and Space Science News, 98. http://dx.doi.org/10.1029/2017EO068775.
- Islam, S. U. I., Dery, S. J., & Werner, A. T. (2017). Future climate change impacts on snow and water resources of the Fraser River basin. *Journal* of *Hydrometeorology*, 18, 473–496.
- Jarvis, S. K., Wiles, G. C., Appleton, S. N., D'Arrigo, R. D., & Lawson, D. E. (2013). A warming-induced biome shift detected in tree growth of mountain hemlock (*Tsuga mertensiana* [bong.] Carrière) along the Guld of Alaska. Arctic, Antarctic, and Alpine Research, 45, 211–218.
- Jost, G. & Weber, F. A. (2012). Potential impacts of climate change on BC Hydro's water resources (BC Hydro Report). Retrieved from http:// www.bchydro.com/content/dam/hydro/medialib/internet/ documents/about/climate_change_report_2012.pdf
- Kiffney, P. M., Bull, J. P., & Feller, M. C. (2002). Climatic and hydrologic variability in a coastal watershed of southwestern British Columbia. *Journal of the American Water Resources Association*, 38, 1437–1451.
- Koop, S. H. A., Koetsier, L., Doornhof, A., Reinstra, O., Van Leeuwen, C. J., Brouwer, S., ... Driessen, P. P. J. (2017). Assessing the governance capacity of cities to address challenges of water, waste, and climate change. Water Resources Management, 31, 3427–3443.
- Kottek, M., Friser, J., Beck, C., Rudolf, B., & Rubel, F. (2006). World map of the Koppen-Geiger climate classification. *Meteorologische Zeitschrift*, 15, 259–263.
- Kottek Markus, Grieser Jürgen, Beck Christoph, Rudolf Bruno, Rubel Franz (2006). World Map of the Köppen-Geiger climate classification updated. Meteorologische Zeitschrift, 15(3), 259–263. http://dx.doi. org/10.1127/0941-2948/2006/0130.
- Larocque, S. J., & Smith, D. J. (2005). A dendroclimatological reconstruction of climate since AD 1700 in the Mt. Waddington area, British Columbia Coast Mountains, Canada. *Dendrochronologia*, 22, 93–106.
- Littell, Jeremy S, Pederson, Gregory T, Gray, Stephen T, Tjoelker, Michael, Hamlet, Alan F, & Woodhouse, Connie A (2016). Reconstructions of Columbia River streamflow from tree-ring chronologies in the Pacific Northwest, USA. Journal of the American Water Resources Association, 52, 1121–1141.
- MacDonald, G. M., & Case, R. A. (2006). Variations in the Pacific decadal oscillation over the last millennium. Geophysical Research Letters, 32, L08703.

- McAfee Stephanie A. (2014). Consistency and the Lack Thereof in Pacific Decadal Oscillation Impacts on North American Winter Climate. *Journal of Climate*, *27*(19), 7410–7431. http://dx.doi.org/10.1175/jcli-d-14-00143.1.
- McCabe, G. J., & Dettinger, M. D. (2002). Primary modes and predictability of year-to-year snowpack variations in the western united stations from teleconnections with Pacific Ocean climate. *Journal of Hydrome-teorology*, 3, 13–25.
- Meko DM, Woodhouse CA, and Bigio ER (2017) University of Arizona Southern California Tree-Ring Study: Final report (Agreement No. 4600011071). December 31, 2017.
- Mishra, A. K., & Coulibaly, P. (2009). Hydrometric network evaluation for Canadian watersheds. *Journal of Hydrology*, 380, 420–437.
- Moore, R. D., & Kendry, M. (1996). Spring snowpack anomaly patterns and winter climatic variability, British Columbia, Canada. Water Resources Research, 32, 623–632.
- Moore, R. D., Spittlehouse, D. L., Whitfield, P. H., & Stahl, K. (2010). Weather and climate. In R. G. Pike, T. E. Redding, R. D. Moore, R. D. Winkler, & K. D. Bladon (Eds.), Compendium of Forest hydrology and geomorphology in British Columbia Land Management Handbook (Vol. 66, pp. 47–83). Victoria, Canada.B.C. Ministry of Forests and Range Research Branch.
- Mote, P. W., Hamlet, A. F., Clark, M. P., & Lettenmaier, D. (2005). Declining mountain snowpack in western North America. *Bulletin of the American Meteorological Society*, 86, 39–49.
- Mote, P. W., Li, S., Lettenmaier, D. P., Xiao, M., & Engel, R. (2018). Dramatic declines in snowpack in the western US. NPJ Climate and Atmospheric Science, 1, 2.
- NOAA (National Oceanic and Atmospheric Administration). (2017). *Paleoclimatology datasets*. https://www.ncdc.noaa.gov/data-access/paleoclimatology-data
- North, G. R., Bell, T. L., Cahalan, R. F., & Moeng, F. J. (1982). Sampling errors in the estimation of empirical orthogonal functions. *Monthly Weather Review*, 110, 699–706.
- Olmstead, S. M. (2014). Climate change adaptation and water resource management: A review of the literature. *Energy Economics*, 46, 500–509.
- Panthi, S., Brauning, A., Zhou, Z.-K., & Fan, Z.-X. (2017). Tree rings reveal recent intensified spring drought in the central Himalaya, Nepal. Global and Planetary Change, 157, 26–34.
- Pederson, G. T., Gray, S. T., Woodhouse, C. A., Betancourt, J. L., Fagre, D. B., Littell, J. S., ... Graumlich, L. J. (2011). The unusual nature of recent snowpack declines in the North American cordillera. *Science*, 333, 332–335.
- Peterson, D. W., & Peterson, D. L. (2001). Mountain hemlock growth responds to climatic variability at annual and decadal time scales. *Ecology*, 82, 3330–3345.
- Pitman, P. J., & Smith, D. J. (2012). Tree-ring derived little ice age temperature trends from the Central British Columbia Coast Mountains, Canada. Quaternary Research, 78, 417–426.
- Pojar, J., Klinka, K., & Meidinger, D. V. (1991, February). *Ecosystems of British Columbia* (Special Report Series 6). BC Ministry of Forests.
- River Forecast Centre. (2017). Snow conditions and water supply bulletin.

 River Forecast Centre. https://catalogue.data.gov.bc.ca/dataset/705df46f-e9d6-4124-bc4a-66f54c07b228
- Rodenhuis, D., Bennett, K. E., Werner, A. T., Murdock, T. Q., & Bronaugh, D. (2009). Climate overview 2007: Hydro-climatology and future climate impacts in British Columbia, Victoria, British Columbia: . Pacific Climate Impacts Consortium, University of Victoria 152pp.
- Roesch A and Schmidbauer H (2015, February 19) Computation wavelet analysis: R package "WaveletComp".
- Salas, J. D., Delleur, J. W., Yevjevich, V., & Lane, W. L. (1980). Applied modelling of hydrologic time series. Littleton, CO: Water Resources Publications 484 pp.

- Schweingruber, F. H., Briffa, K. R., & Jones, P. D. (1991). Yearly maps of summer temperatures in Western Europe from AD 1750 to 1975 and Western North America from 1,600 to 1982: Results of a radiodensitometrical study on tree rings. Vegetation, 92, 5-71.
- Sellars, C. D., Garret, M., & Woods, S. (2008). Influence of the Pacific decadal oscillation and El Nino southern oscillation on the operation of the Capilano water supply reservoir, Vancouver, British Columbia. Canadian Journal of Water Resources, 33, 155–164.
- Speer, J. H. (2010). Fundamentals of tree ring research. Tucson: University of Arizona Press 368 pp.
- Spry, C. M., Kohfeld, K. E., Allen, D. M., Dunkley, D., & Lertzman, K. (2014). Characterizing pineapple express storms in the lower mainland of British Columbia, Canada. *Canadian Water Resources Journal*, 39, 302–323.
- Stahl, K., Moore, R. D., & Mckendry, I. G. (2006). The role of synoptic-scale circulation in the linkage between large-scale ocean-atmosphere indices and winter surface climate in British Columbia, Canada. *Interna*tional Journal of Climatology, 26, 541–560.
- Thakur, B., Kalra, A., Lakshmi, V., Lamb, V. W., Miller, W. P., & Tootle, G. (2020). Linkage between ENSO phases and western US snow water equivalent. *Atmospheric Research*, 236, 104827.
- Welsh, C., Smith, D. J., & Coulthard, B. (2019). Tree-ring records unveil long-term influence of the Pacific decadal oscillation on snowpack dynamics in the Stikine River basin, northern British Columbia. *Hydrological Processes*, 33, 720–736.
- Whitfield, P. H., Moore, R. D., Fleming, S. W., & Zawadzki, A. (2010).
 Pacific decadal oscillation and the hydroclimatology of western
 Canada Review and prospects. Canadian Water Resources Journal,
 35, 1–28.
- Wiles, G., Jacoby, G. C., & Davi, N. K. (1999). NOAA/WDS paleoclimatology

 Wiles Deer Mountain TSME ITRDB AK098. Retrieved from https://www.ncdc.noaa.gov/paleo/study/12445.
- Wolter, K. & Timlin, M. S. (1993). Monitoring ENSO in COADS with a seasonally adjusted principal component index. Paper presented at the Proceedings of the 17th Climate Diagnostics Workshop, Norman, OK: NOAA/NMC/CAC, NSSL, Oklahoma Climate Survey, CIMMS, and the School of Meteorology.
- Wolter, K., & Timlin, M. S. (2011). El Niño/southern oscillation behaviour since 1871 as diagnosed in an extended multivariate ENSO index (MEI.Ext). International Journal of Climatology, 31, 1074–1087.
- Wong, T.-. T. (2015). Performance evaluation of classification algorithms by k-fold and leave-one-out cross validation. *Pattern Recognition*, 48, 2839–2846.
- Woodhouse Connie A., Pederson Gregory T., Morino Kiyomi, McAfee Stephanie A., McCabe Gregory J. (2016). Increasing influence of air temperature on upper Colorado River streamflow. *Geophysical Research Letters*, 43(5), 2174–2181. http://dx.doi.org/10.1002/ 2015gl067613.
- Wood, L. J., Smith, D. J., & Demuth, M. N. (2011). Extending the place glacier mass-balance record to AD 1585, using tree rings and wood density. *Quaternary Research*, 76, 305–313.
- Yu, B., & Zwiers, F. W. (2007). The impact of combined ENSO and PDO on the PNA climate: A 1,000-year climate modelling study. *Climate Dynamics*, 29, 837–851.

How to cite this article: Mood BJ, Coulthard B, Smith DJ. Three hundred years of snowpack variability in southwestern British Columbia reconstructed from tree-rings. *Hydrological Processes*. 2020;34:5123–5133. https://doi.org/10.1002/hyp.13933